Time Decay of the Activity of the Reduction Reaction of NO by CO on a Pd/Al_2O_3 Catalyst

Joaquín Cortés · Eliana Valencia · Gonzalo Aguila · Esteban Orellana · Paulo Araya

Abstract An experimental study is made of the time decay of activity of the CO–NO reaction on a Pd/Al_2O_3 looking at the effect on reaction order and apparent activation energy. The optimum kinetics parameters fitting the steady state data at moderate pressures are determined. The time decay curves are analyzed through various catalyst deactivation models.

Keywords Catalysis · CO–NO reaction over palladium · Decay of the catalytic activity

1 Introduction

Over the last decades great progress has been made in the knowledge of superficial catalytic reactions. This has been due on the one hand to modern laboratory techniques and on the other to a better understanding of the behavior of irreversible dynamic systems of which superficial reactions are an example. These kinds of systems have called the joint attention of chemists because of their applications in catalysis and of physicists because they are good examples of nonequilibrium models that show interesting complex phenomena such as oscillations, kinetics phase transitions, hysteresis, chaos, dissipative structures, etc [1]. These aspects have also been reviewed very appropriately by Evans [2], Zhdanov [3] and Albano [4].

A particularly interesting example of a superficial reaction has been the catalytic reduction of NO by CO (CO–NO reaction) over a variety of noble and transition metals, which together with the oxidation reaction of CO have been studied extensively, especially because of their importance in the catalytic removal of pollutants such as nitrogen oxides (NO_x) produced in the exhaust gases of automobiles after the introduction in the late 1970s of the three-way catalytic converter [5].

In recent years there has been growing interest in studying the catalytic behavior of palladium in the CO–NO reaction, with the purpose of replacing rhodium in automobile converters, in which, together with platinum, it shows outstanding efficiency. This is not only due to its lower cost because of its greater abundance in nature, but also because, in addition to having good behavior in the oxidation of hydrocarbons, it has greater resistance to being sinterized at high temperatures. Improvements in the purification of gasoline, on the other hand, have decreased the problem of the lower resistance shown by Pd, compared to the other noble metals, to poisoning with S and Pb.

In the literature, experimental information on the kinetics of the CO–NO reaction over palladium is scarcer than on rhodium, and it is also more controversial, in part because of the different conditions and experimental techniques that have been used. For example, Reiner et al. [6, 7] and Holles et al. [8, 9] have published data obtained from a conventional flow reactor, while Prevot et al. [10, 11], Nakao et al. [12] and Thirumoorthy et al. [13] used molecular beam techniques.

In this paper we are interested in studying the CO–NO reaction over palladium supported on alúmina, considering the dispersed information reported for this system, such as that of Holles et al. [9] that we will comment below. Our main interest, however, which is probably related to the above, is the deactivation over time that this system undergoes during the process of the reaction, making it difficult to achieve the steady state. According to the

J. Cortés (✉) · E. Valencia · G. Aguila · E. Orellana · P. Araya
Facultad de Ciencias Físicas y Matemáticas, Universidad de Chile, Casilla 2777, Santiago, Chile
e-mail: jcortes@dqb.uchile.cl

literature and to our laboratory experience [14], this phenomenon does not occur with rhodium. As far as the authors are aware, this situation, which can be seen in the figures in the next section, has only been commented incidentally in a recent paper by Reiner et al. [7].

Additional interest in the chosen system refers to the reaction mechanism. The delay in research with Pd catalysts with respect to that with Rh and Pt has meant a greater uncertainty about the microscopic behaviour reflected in the kinetics mechanism, in the case of the CO–NO reaction on Pd, as mentioned recently [10–13]. However, the closeness of these three metals in the periodic table may hint that the mechanism should not be too different for all of them. This explains why there have been recent attempts to associate the mechanism on Pd with the previously known mechanisms on Rh for the same reaction [10–13].

The mechanism on Rh has a long and conflicting history since the early work of Hecker and Bell [15], followed by, among others, the work of Oh [16], Cho [17], Chuang and Tan [18], Peden et al. [19] and Permana et al. [20], and that from our laboratory [14, 21], where we have considered recent experiments by Zaera's group [22]. In view of the attractive matters discussed previously with respect to this mechanism, included also in a large number of theoretical papers, with some contributions from our laboratory [23], it seems appropriate to make use of the recent interest in Pd as a catalyst to extend those studies. This will allow a better understanding of the microscopic behaviour of this interesting reaction whose possible applications have incentivated current interest.

In view of the above considerations, this paper will report on the experimental study of the deactivation over time seen in the kinetics of the CO–NO reaction on a Pd/Al_2O_3 catalyst under moderate pressure. On the other hand, assuming elemental stages similar to those proposed previously for Rh, the reaction's kinetics constants and the behaviour of the production curves and the phase diagrams will be examined, and the experimental deactivation curves will be contrasted with those found for some of the most representative deactivation models of catalysts reported in the literature.

2 Experimental Procedure

A 2% Pd/Al_2O_3 catalyst was prepared by impregnating γ-Al_2O_3 (BAFF) with an appropriate amount of aqueous solution of $Pd(NO_3)_2$ (Merck). The impregnated support was then dried in an oven at 105 °C during 12 h. The dispersion initial of the catalyst before the reaction, determined by chemisorption of hydrogen, was equal to 18.4%. The dispersion was also determined after the reaction at various temperatures, finding that its value does not change significantly during the process of the reaction, an aspect that will be commented later.

To determine the catalytic activity, 0.1 g of catalyst were loaded into a 50-cm long and 1-cm diameter tubular reactor. The catalyst was calcined in situ during 1 h at 500 °C in a 10 cm^3/min stream of pure O_2, cooled to 300 °C, and reduced in a flow of 30 cm^3/min of a 5% H_2/Ar stream during 1 h. After that, the feed was switched to pure He and maintained at 300 °C for 1 h. The reactor temperature was then decreased to room temperature and the reactants were allowed to flow (90 cm^3/min) at a concentration of 1.55% CO and 0.23% NO, the balance He, corresponding to 11.78 Torr of CO and 1.748 Torr of NO. The temperature was then increased using an RKC model REX-P100 programmer at a rate of 2 °C/min until the desired working temperature was reached. The reactor inlet and outlet streams were analyzed by gas chromatography using two Perkin Elmer Autosystem chromatographs equipped with HWD detectors. The first chromatograph had a HAYASEP D (2 m × 1/8 inch) column to analyze CO_2 and N_2O, and the second had an MS 5A (1 m × 1/8 inch) column to analyze CO. The conversion of NO and CO was calculated from the C and N mass balance, considering that the only nitrogen-containing products are N_2 and N_2O, and the only carbon-containing product is CO_2, according to the following reaction pathways:

$$CO + 2NO = CO_2 + N_2O \quad (1)$$

$$CO + NO = CO_2 + {}^1/_2N_2 \quad (2)$$

Therefore, the N_2 concentration ($[N_2]$) was estimated from the equation:

$$[N_2] = {}^1/_2\left([CO_2]_t - [N_2O]_t\right) \quad (3)$$

where $[CO_2]_t$ and $[N_2O]_t$ are the CO_2 and N_2O concentrations, respectively, in the reactor effluent.

3 Experimental Results

Figure 1a shows the curves of the conversion rate of NO and CO and the formation rate of N_2 and N_2O versus time in the case of a temperature equal to 493 K and the Fig. 1b shows the variation over time of the activity of the CO–NO reaction on Pd/Al_2O_3 at different temperatures, measured in TON frequencies for CO conversion based on the measurements of dispersion determined by hydrogen chemisorption. Since in all cases conversion remained at values below 10%, it is possible to use, assuming a plug-flow reactor, the following approximate expression to relate the activity R_{CO_2} (TON) with the conversion X_{CO}

$$R_{CO_2} = \frac{F_{CO}X_{CO}}{N_{Pd}} \quad (4)$$

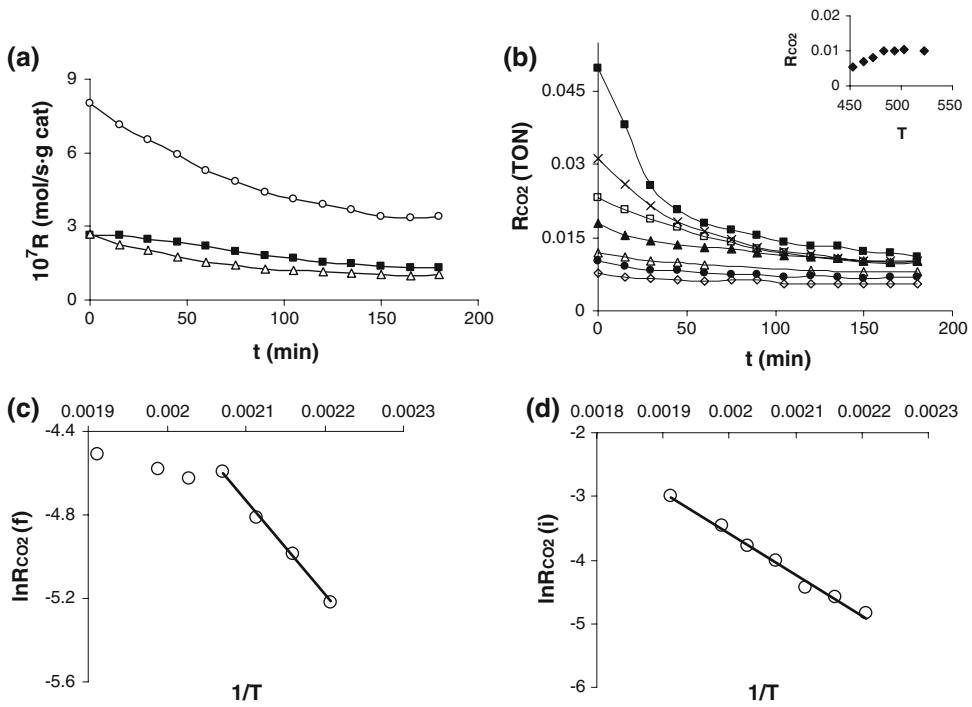

Fig. 1 (**a**) R(mol/s g cat.): CO (○) conversion rate and N_2 (Δ) and N_2O (■) formation rate at 493 K. (**b**) Activity TON (molecules/site s) decay over time for the CO–NO reaction on Pd/Al_2O_3 at various temperatures (◇) 453 K (●) 463 K (Δ) 473 K (▲) 483 K (□) 493 K (X) 503 K (■) 523 K. The inset shows an enlargement of the final steady state. The lines have been drawn to guide the eyes. (**c**) Arrhenius-like expression in the final steady state. (**d**) The same as (**c**) in the initial state of the process (t = 0)

where N_{Pd} represents the number of Pd sites on the surface and F_{CO} is the CO flow into the reactor.

The observed deactivation is high at high temperatures, reaching 78% of the initial activity at 523 K, a value similar to that of Rainer et al. [7], who report a decrease "by a factor of 5 or more" in the 540–580 K temperature range. At lower temperatures, however, deactivation decreases substantially, reaching 27% of its initial value at 453 K.

At all the temperatures used, after 3 h an activity was achieved whose later variation was marginal for the objectives of the experiment, so it was considered that the steady state had been reached. In Fig. 1c it is seen that for steady state values a good Arrhenius straight line is obtained in the lower temperature range, with an apparent activation energy of 8.9 (kcal/mol), a low value compared to others reported in the literature for the same system. The same equation was used to fit the points of the zone corresponding to the initial time of the experiments. In this case in Fig. 1d it is seen that the Arrhenius straight line is fulfilled with a high correlation in the temperature interval studied, getting a high apparent activation energy equal to 12.8 (kcal/mol). It is interesting to note that for the same system a wide spectrum of values has been reported for the apparent activation energy [6, 7, 24, 25], as pointed out by Holles et al. [9], who give values that vary between 10.2 and 14.3 (kcal/mol) for various catalyst loads. These activation energies are of the same order as those obtained in our experiments.

Figure 2 shows the results obtained for order m with respect to CO and n with respect to NO defined by the expression

$$R_{CO_2} = kP_{CO}^{m}P_{NO}^{n} \quad (5)$$

The values of m and n have been determined at 453 K, which corresponds to the lowest temperature of Fig. 1b, at which the lowest activity decrease is seen, 27% after 3 h of process. Figure 2 shows the evolution over time at 453 K under different CO and NO pressures, keeping one of them constant and the curves of Eq. 5 linearized to obtain parameters m and n, considering the initial and final steady state values in both cases. The negative order with respect to CO and positive for NO, agrees in the steady state case with those reported by Holles et al. [8, 9] and with those of Reiner et al. [7] for the same system. On the other hand, the increase of the negative parameter value for CO and the decrease of the positive parameter with respect to NO between the initial states and the steady state, reflect the system's deactivation through a decrease of R_{CO_2} according to Eq. 5.

4 Discussion

4.1 The Reaction Mechanism and the Kinetics Parameters

As has been mentioned [10, 13], the microscopic behavior of the kinetics of the CO–NO reaction on Pd is not fully

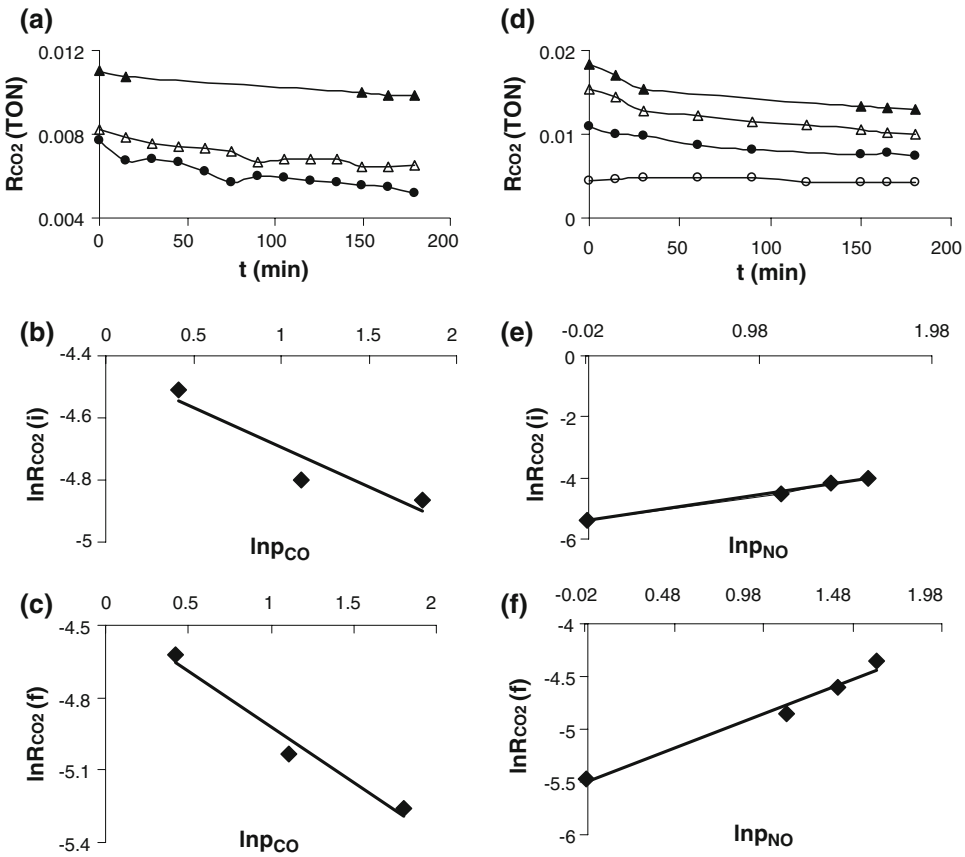

Fig. 2 (**a**) Activity decay over time curves for the CO–NO reaction on Pd/Al_2O_3 at 453 K and various CO pressures in the gas phase (●) $p_{CO} = 6.08$ Torr; (Δ) $p_{CO} = 3.04$ Torr; (▲) $p_{CO} = 1.52$ Torr. The lines have been drawn to guide the eyes. (**b**) ln CO_2 production as a function of ln CO pressure with a fixed NO pressure of 1.748 Torr at 453 K in the initial state (t = 0). (**c**) The same as (**b**) in the final steady state. (**d**) The same as (**a**) at 453 K and various NO pressures in the gas phase $p_{NO} = 0.99$ Torr (▲); $p_{NO} = 3.04$ Torr (Δ); $p_{NO} = 4.03$ Torr (●); $p_{NO} = 5.02$ Torr (○). (**e**) The same as (**b**) as a function of NO pressure with a fixed CO pressure of 6.08 Torr. (**f**) The same as (**e**) in the final steady state

understood. However, because of the closeness in the periodic table, a reaction mechanism similar to that of Langmuir Hinshelwood (LH) used by Cortés et al. [26] and Zhdanov and Kasemo [27] for the same reaction on Rh has recently been proposed by various authors as probable [10–13]. This mechanism, whose elemental stages appear in Scheme 1, has been used in this paper.

The use of the kinetics equations of a given mechanism to interpret the experimental information requires in the

(1) $CO + S \xrightarrow{k_1} CO_{(a)}$

(2) $CO_{(a)} \xrightarrow{k_2} CO + S$

(3) $NO + S \xrightarrow{k_3} NO_{(a)}$

(4) $NO_{(a)} \xrightarrow{k_4} NO + S$

(5) $NO_{(a)} + S \xrightarrow{k_5} N_{(a)} + O_{(a)}$

(6) $2N_{(a)} \xrightarrow{k_6} N_2 + 2S$

(7) $CO_{(a)} + O_{(a)} \xrightarrow{k_7} CO_2 + 2S$

(8) $NO_{(a)} + N_{(a)} \xrightarrow{k_8} N_2O + 2S$

Scheme 1 Mechanism of the CO–NO reaction used in the paper

first place the determination of the value of the rate constants k_i. The determination of these parameters from the experimental data is a matter of permanent interest that has been discussed frequently in the literature. Two situations have been stressed in this relation. The first has to do with the difficulty to interpret kinetics information in the moderate and high pressure zones with data obtained in the zone of very low pressure or ultra high vacuum (UHV). This has been called the pressure-gap problem [11] and has been discussed in detail by Zhdanov [28] for example, in the case of the CO–NO reaction on Rh, with rather discouraging results. The other situation is the difficulty to interpret the results of kinetics experiments over technical catalysts of great material complexity, such as supported catalysts, with parameters obtained over single crystals whose simplicity guarantees better reproducibility of the results. This situation has been called the "material gap problem" [11].

The above considerations have given rise to our interest in attempting some analyses comparing the analytic solution of the previous mechanism with the information that we have obtained in the steady state zone for the CO–NO reaction over palladium, considering that in the literature on the subject, as far as the authors are aware, no values have been reported for these parameters at moderate or

high pressures, except for a partial fit in a paper from our laboratory [29]. Only in two recent articles there are proposals for a set of kinetics parameter values for the reaction in question on Pd [10, 12] that have been determined experimentally using a molecular beam reaction system in the low pressure and UHV zones, showing only the appearance of CO_2 and N_2 as products. For that reason, both cases considered a mechanism like that of Scheme 1, but excluding step (8), the formation of N_2O.

With that purpose we have determined a set of kinetics parameters for the system of concern. These are the optimum activation energy values and frequency factors of the mechanism's steps, corresponding to the values that minimize function ϕ. The procedure took into account all the experimental data in the final steady state at the various pressures and temperatures of Figs. 1 and 2. Function ϕ is given by the expression:

$$\phi = \sum \left[\frac{R_{CO_2}(t) - R_{CO_2}(e)}{R_{CO_2}(e)}\right]_i^2 + \left[\frac{R_{N_2}(t) - R_{N_2}(e)}{R_{N_2}(e)}\right]_i^2 + \left[\frac{R_{N_2O}(t) - R_{N_2O}(e)}{R_{N_2O}(e)}\right]_i^2 \quad (6)$$

where i represents each of the points in the steady state, $R_j(t)$ is the theoretical production of product (j), and $R_j(e)$ is the corresponding experimental value.

Considering that the adsorption steps are not activated and their kinetics constants are calculated according to the expression (7) of the kinetic theory of gases it is necessary to optimize a total of 12 parameters.

$$k_i(ads) = S_i\sigma(2\pi M_i RT)^{-1/2} \quad (7)$$

M_i is the molecular mass of i, S_i is the corresponding sticking coefficient, which we have taken to be equal to 1 in this paper, and the coefficient σ is the area occupied by 1 mol of superficial metal atoms. However, and since after attempting various optimization attempts it was not possible to adjust the parameters corresponding to step (7), CO_2 production, those parameters were set equal to those obtained by Nakao et al. [12], optimizing the 10 remaining parameters. The results obtained are shown in Table 1 and the fit can be visualized in Fig. 3 for the productions and selectivities for N_2 at various temperatures.

It was necessary to set up an analytical expression for the solution of the kinetics of the mechanism proposed in Scheme 1 to obtain the optimum parameters shown in Table 1. This is not possible if all the mass balances are established, because in this case numerical solutions can only be obtained point by point. Fortunately, as shown in Appendix A, analytic solutions can be found for the covering using the approximation that assumes an equilibrium between the adsorbed species CO(a) and NO(a) and their molecules in the gas phase. This approximation, which we have used before [14, 21, 26] and which assumes high adsorption and desorption rates, is reasonable within the working range of the paper, as has been commented in the literature for the CO–NO [12] reaction. The validity of the approximation has also been confirmed in one of our previous works using Monte Carlo simulations [21] and by numerical integration of the mass balance equations [14]. In that work it was found an excellent agreement between the analytical approximation, Appendix A, and the numerical solution.

Table 1 Kinetics parameters used in the paper

Event	Activation energy E_i (kcal/mol)	Frecuency factor ν_i (s^{-1})
CO desorption	30.7	1.37×10^{21}
NO desorption	32.8	5.22×10^{22}
NO dissociation	29.3	7.65×10^{13}
CO_2 production[a]	33.6	7.10×10^{15}
N_2 production	25.7	1.20×10^{11}
N_2O production	35.8	2.27×10^{17}

[a] Ref. [12]

In addition to provide a set of kinetics parameters at moderate pressures for the CO–NO reaction over supported palladium, the result is interesting because it allows the observation, through an optimum fit of the experimental information, beside the production diagram at various temperatures and concentrations of the gas phase, of what happens in the adsorbed phase through the phase diagram, under a given mechanism. Figure 3 is a graph of production and coverage of the different superficial species versus temperature, in the range of the experiments performed, and versus the CO concentration, y_{CO}, in the gas phase assuming a total pressure equal to 10 Torr, obtained from the analytic equations of the mechanism of Scheme 1 (Appendix A) and the parameters of Table 1. The production versus temperature diagram includes the values from our experiments to visualize the result of the fit.

It is seen that the production versus temperature and concentration diagrams present a maximum. This situation has also been seen in the work of Nakao et al. [12] and Prévot et al. [10] with data in the low pressure zone. The phase diagram, on the other hand, shows a growth of CO coverage with concentration y_{CO} due to the increased adsorption of CO, which also has the linear shape seen by Nakao at low pressures. This increase of θ_{CO} accounts for the strongly decreasing shape of the curve corresponding to the oxygen coverage which is consumed by CO according to step (7). This, which accounts for the growth of the production curve, has a limit at high CO coverage where θ_O decreases markedly, thereby decreasing production and accounting for the maximum of the curve.

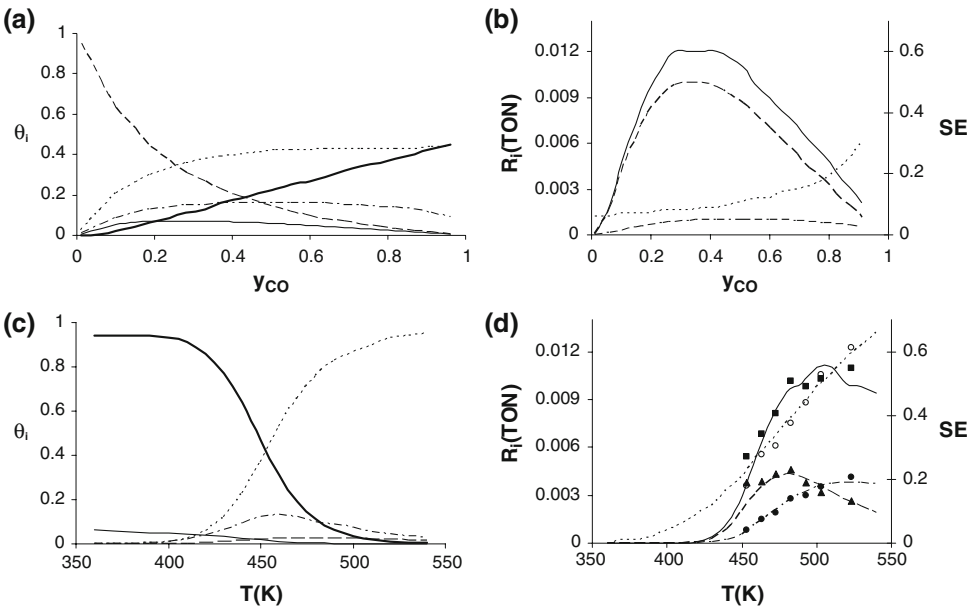

Fig. 3 Theoretical curves corresponding to the Scheme 1 mechanism with the parameters of Table 1. (**a**) Phase diagram at 453 K —— (θ_{CO}) - - - - (θ_O) ····· (θ_S) · — · — · — (θ_N) —— (θ_{NO}). (**b**) Production diagram and selectivity at 453 K versus y_{CO} — (R_{CO_2}); - - - - (R_{N_2O}); — · — · — (R_{N_2}); ····· (SE). (**c**) The same as (**a**) versus T at $p_{CO} = 11.78$ Torr and $p_{NO} = 1.748$ Torr. (**d**) The same as (**b**) at $p_{CO} = 11.78$ Torr and $p_{NO} = 1.748$ Torr. The experimental points are the steady state values of Fig. 1. ■ (R_{CO_2}); ▲ (R_{N_2O}); ● (R_{N_2}); ○ (SE)

At low temperature the surface is poisoned with CO and a small fraction of NO, hindering production, which is only possible at higher temperatures at which CO desorption allows an increase of vacant sites, the reaction of step (7) taking place with the superficial oxygens produced by the dissociation of NO. These oxygens remain as a small fraction under the pressure conditions of the figure, due to the existence of a large amount of superficial CO, except in the high temperature zone where θ_{CO} tends to decrease causing a decrease of the activity in the production curves.

4.2 Catalyst Deactivation Models

One of the most insidious problems of catalysis is the loss of catalytic activity that occurs as the reaction takes place on the catalyst. The complexity of the phenomenon, which makes it difficult to tackle because of the multiple possible causes that can explain it, is certainly the reason why it has not been sufficiently dealt with in the more recent literature on the subject. However, a number of models have been proposed, some of them of a more empirical character and others corresponding to various deactivation mechanisms.

Our results confirm that the decay in the activity has to do with situations related to the behavior of the reaction rather than to changes in the catalyst's structure. As mentioned in a previous section, the dispersion did not undergo a significant variation of its values determined before and after the reaction. It was also found that if the reaction process was repeated using the same catalyst, the previous decay curve was reproduced. Both aspects indicate that within the pressure and temperature range studied the decay of the reaction was not due to changes undergone by the solid's surface. This is also in agreement with the results reported by Rainer et al. [6, 7] for the same system in the (512–588 K) range using TEM, where they do not find qualitative changes in particle size distribution between reacted and unreacted catalysts.

Table 2 shows some cases of models for the activity decay that we have considered as the most representative to interpret our experimental data, such as Eq. 8, whose linear shape is the simplest possible [30], a hyperbolic law represented by Eq. 9 that has been proposed in case the deactivation is due to aging by sinterizing of the catalytic substrate [31], Eq. 10 which corresponds to an exponential law proposed in some cases of poisoning by molecules that are irreversibly chemisorbed on the surface [34], and expression (11), proposed in some examples of coking or dirtying of the surface [35]. In all cases the decay of CO_2 production has been expressed through the normalized variable at the initial time $A = R_{CO_2}(t = t)/R_{CO_2}(t = 0)$.

The table shows, for some temperatures, the optimum parameters of the corresponding equation and the value of the quadratic function ϕ for each of the minima, given by the expression $\phi = \sum (R_{CO_2}(t)_i - R_{CO_2}(e)_i)^2$. It is seen that in the case of our experimental data the best fit with the model is given by Eq. 11. Figure 4 shows the good interpretation of the experimental points by the model represented by Eq. 11.

Even though we do not believe that the fit with theoretical models must be considered as a definitive viewpoint in relation to the decay experiments that we are studying, it is interesting to comment in that respect the observations of Reiner et al. [7] in the case of this system. While those authors do not report data of decay curves, they state that

Table 2 Fitting parameters of the corresponding models and some experimental data of Fig. 1a

T	K_1	ϕ		
463	0.00239	0.0603	$A = 1 - K_1 t$	(8)
483	0.00304	0.0705	Linear [30]	
493	0.00397	0.0731		
503	0.00487	0.229		
T	K_2	ϕ		
463	0.00373	0.0261	$A = \frac{1}{1+K_2 t}$	(9)
483	0.00539	0.0171	Hyperbolic [31]	
493	0.00852	0.0024		
503	0.0143	0.0050		
T	K_3	K_4	ϕ	
463	0.0021	0.91	0.0174	$A = K_3 \exp(-K_4 t)$ (10)
483	0.0032	0.91	0.0152	Exponential [34]
493	0.0055	0.96	0.0114	
503	0.0075	0.91	0.0360	
T	K_5	K_6	ϕ	
463	0.0342	0.53	0.00182	$A = \frac{1}{1+K_5 t^{K6}}$ (11)
483	0.0258	0.66	0.000889	[35]
493	0.0072	1.04	0.00234	
503	0 .0198	0.926	0.00374	

they have observed the phenomenon in their experiments, commenting that a possible cause may be the blocking of sites by carbon atoms produced by the dissociation of CO that some authors [35] have shown to be produced on small particles of supported Pd under some conditions. This argument can account for the better fit of Eq. 11 with our data because it would correspond to a model of deactivation by coking of the surface.

Another possible explanation of the phenomenon given by Rainer et al. [7] is the presence of inactive nitrogen atoms adsorbed on the surface, like those proposed by Oh and Eickel [16] to explain the behaviour of the system in the case of rhodium. However, it is not a simple matter to associate this case with a given decay equation.

Since an increase of the parameters should decrease the value of ϕ, it is not simple to compare Eqs. 9 and 11, which correspond, respectively, to sintering and coking. However, the case of sintering should be excluded because, as commented by Rainer et al. [7], production decay cannot be due to a sintering effect of the material because the catalyst "has been exposed to much harsher temperature conditions during initial reduction than it experiences in the CO–NO run." This has also been the case in our experiments.

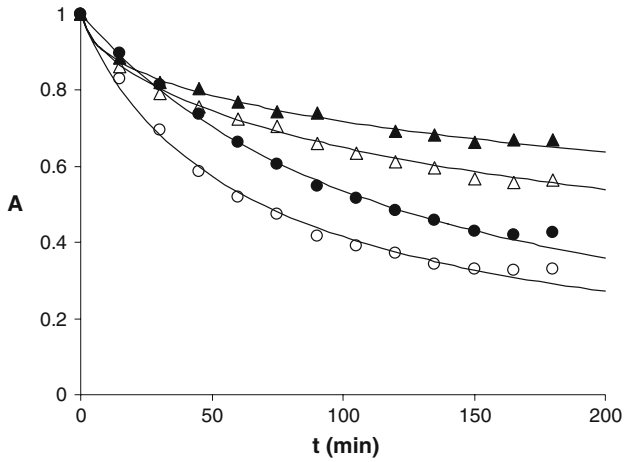

Fig. 4 Decay of normalized production $A = R_{CO_2}(t)/R_{CO_2}(t = 0)$ versus time. (▲) 463 K; (Δ) 483 K; (●) 493 K; (○) 503 K. The lines correspond to the deactivation model of Eq. 11 of Table 2

5 Conclusions

1. The experimental activity decay over time curves for the CO–NO reaction on Pd/Al_2O_3 were determined at various pressures and temperatures. The apparent activation energies and reaction orders with respect to CO and NO at the start of the process and the final steady state are coherent with that decay.
2. The experimental activity decay over time curves were contrasted with catalyst deactivation models reported in the literature. The model that best fits the experimental data is that of superficial dirtying or coking".
3. It is confirmed that the activity decay is related to situations having to do with the behavior of the reaction rather than with changes in the catalyst's structure, because no significant changes are seen in the value of the dispersion before and after the reaction, and the decay curves are reproduced if the same catalyst is used.
4. A set of kinetics parameters for this system at moderate pressures was established, assuming a mechanism similar to one reported previously for the same reaction over rhodium. The production versus temperature and gas phase concentration curves show a maximum similar to that reported for low pressures, which is accounted for by the behaviour of the adsorbed phase seen in the phase diagrams.

Acknowledgments The authors acknowledge the financial support of this work by FONDECYT under Project 1070351.

Appendix A: Analytic Solution of the Reaction Model Used in the Paper

In a manner similar to the development shown in one of our previous papers [14, 21, 26], we will synthetize the equations used in this paper for the mechanism of Scheme 1. Since it is assumed that the $CO_{(a)}$ and $NO_{(a)}$ adsorbates are in equilibrium with the gas phase, it is possible to write the relations:

$$K_{CO} = \frac{\theta_{CO}}{\theta_S P_{CO}} \quad K_{NO} = \frac{\theta_{NO}}{\theta_S P_{NO}} \tag{A1}$$

where the equilibrium constants are expressed as functions of the coverages θ_{CO} and θ_{NO}, and the partial pressures P_{CO} and P_{NO} of the gas phase, and θ_S represents the coverage of the vacant surface sites. The procedure used consists in expressing the coverages θ_i as functions of θ_{CO}, for which, if we define

$$A = \frac{P_{NO} K_{NO}}{P_{CO} K_{CO}} \tag{A2}$$

$$B = \frac{1}{P_{CO} K_{CO}} \tag{A3}$$

it is possible to write the relations:

$$\theta_{NO} = A\theta_{CO} \quad \theta_S = B\theta_{CO} \tag{A4}$$

The following conservation equations can be written, where the first two represent the steady state for the surface species $N_{(a)}$ and $O_{(a)}$ $\left(\frac{d\theta_N}{dt} = 0 \quad \text{and} \quad \frac{d\theta_O}{dt} = 0\right)$:

$$k_5\,\theta_{NO}\,\theta s - 2k_6\theta_N^2 - k_8\theta_{NO}\theta_N = 0 \tag{A5}$$

$$k_5\,\theta_{NO}\,\theta_S - k_7\theta_{CO}\theta_O = 0 \tag{A6}$$

$$\theta_S + \theta_{CO} + \theta_{NO} + \theta_N + \theta_O = 1 \tag{A7}$$

If we define the relations

$$C = \left(-k_8 A + \left((k_8 A)^2 + 8k_5 k_6 AB\right)^{1/2}\right) \Big/ 4k_6 \tag{A8}$$

$$D = k_5 AB/k_7 \tag{A9}$$

it is possible to write:

$$\theta_N = C\theta_{CO} \quad \theta_O = D\theta_{CO} \tag{A10}$$

so that from (A7) we have

$$\theta_{CO} = 1/(1 + A + B + C + D) \tag{A11}$$

Therefore the productions R_i are the following:

$$R_{CO_2} = k_7\theta_{CO}\theta_O \quad R_{N_2} = k_6\theta_N^2 \quad R_{N_2O} = k_8\theta_{NO}\theta_N \tag{A12}$$

and the selectivity SE for the nitrogen is defined by

$$SE = R_{N_2}/(R_{N_2} + R_{N_2O}). \tag{A13}$$

References

1. (a) Nicolis G, Prigogine I (1977) Self-organization in nonequilibrium systems. Wiley Interscience, New York; (b) Haken H (1977) Synergetics. Springer-Verlag, New York; (c) Marro J, Dickman R (1999) Nonequilibrium phase transitions in lattice models. University Press, Cambridge
2. Evans JW (1991) Langmuir 7:2514
3. Zhdanov VP, Kasemo B (1994) Surf Sci Rep 20:111
4. (a) Albano EV (1996) Heterog Chem Rev 3:389; (b) Albano EV, Borowko M (2000) Computational methods in surface and colloid science, Chap. 8. Marcel Dekker, New York, pp 387–437
5. (a) Taylor KC (1993) Catal Rev Sci Eng 457:35; (b) Shelef M, Graham G (1994) Catal Rev Sci Eng 36:433
6. Rainer DR, Vesecky SM, Koranne M, Oh WS, Goodman DW (1997) J Catal 167:234
7. Rainer DR, Koranne M, Vesecky SM, Goodman DW (1997) J Phys Chem B 101:10769
8. Holles JH, Davis RJ, Murray TM, Howe JM (2000) J Catal 195:193
9. Holles JH, Switzer MA, Davis RJ (2000) J Catal 190:247
10. Prévot G, Henry CR (2002) J Phys Chem B 106:12191
11. Prévot G, Meerson O, Piccolo L, Henry CR (2002) J Phys Condens Matter 14:4251
12. (a) Nakao K, Ito S, Tomishige K, Kunimori K (2005) J Phys Chem B 109:17579; (b) Olsson L, Zhadanov VP, Kasemo B (2003) Cat Lett 529:338
13. Thirunavukkarasu K, Thirumoorthy K, Libuda J, Gopinath Ch (2005) J Phys Chem B 109:13272
14. Cortés J, Valencia E (2004) J Phys Chem B 108:2979
15. Hecker WC, Bell AT (1983) J Catal 84:200
16. (a) Oh SH, Fisher GB, Carpenter JE, Wayne D (1986) J Catal 100:360; (b) Oh SH, Eickel CC (1991) J Catal 128:526
17. (a) Cho BK (1992) J Catal 138:255; (b) (1994) J Catal 148:697
18. Chuang S, Tan C (1998) J Catal 173:95
19. Peden C, Belton D, Schmieg SJ (1995) J Catal 155:204
20. (a) Permana H, Simon K, Peden C, Schmieg SJ, Belton D (1995) J Phys Chem 99:16344; (b) Permana H, Simon K, Peden C, Schmieg SJ, Lambert DK, Belton D (1996) J Catal 164:194
21. Cortés J, Valencia E (2006) J Phys Chem B 110:7887
22. (a) Zaera F, Gopinath ChS (1999) J Chem Phys 111:8088; (b) Zaera F, Gopinath ChS (2000) Chem Phys Lett 332:209; (c) Zaera F, Gopinath ChS (2002) J Chem Phys 116:1128
23. (a) Cortés J, Puschmann H, Valencia E (1996) J Chem Phys 105:6026; (b) Cortés J, Puschmann H, Valencia E (1998) J Chem Phys 109:6086; (c) Dickman A, Grandi BC, Figueiredo W, Dickman R (1999) Phys Rev E 59:6361; (d) Valencia E, Cortés J (2000) Surf Sci 470:L109; (e) Cortés J, Valencia E (2002) Physica A 309:26; (f) Cortés J, Valencia E (2004) J Phys Chem B 108:2979
24. Vesecky SM, Chem P, Xu X, Goodman DW (1995) J Vac Sci Technol A 13:1539
25. (a) Butler JD, Davis DR (1976) J Chem Soc Dalton Trans 2249; (b) Xi G, Bao J, Shao S, Li S (1992) J Vac Sci Technol A 10:2351; (c) Graham GW, Logan AD, Shelef M (1993) J Phys Chem 97:5445
26. Cortés J, Valencia E, Herrera J, Araya P (2007) J Phys Chem C 111:7063
27. Zhdanov VP, Kasemo B (1997) Surf Sci Rep 29:31
28. (a) Ogunye AF, Ray WH (1971) Ind Eng Chem Process Des Dev 10:410; (b) Maat HV, Moscou L (1965) In: Proceedings of the 3rd International Congress on Catalysis, North-Holland, Amsterdam, p 1277; (c) Pozzi AL, Rase HF (1958) Ind Eng Chem 50:1075
29. Eley DD, Rideal EK (1941) Proc R Soc London A178:429

30. Kuczynski GC (ed) (1975) Sintering and catalysis, vol 10 materials science research. Plenum Press, NY
31. (a) Pease RN, Steward LY (1925) J Am Chem Soc 47:1235; (b) Weekman VW (1968) Ind Eng Chem Process Des Dev 7:90; (c) Ogunye AF, Ray WH (1970) Ind Eng Chem Process Des Dev 9:619; (d) Ferrauto RJ, Bartholomew CH (1997) Fundamentals of industrial catalysis process. Blackie Academic and Professional, Nueva York
32. (a) Voorhies A (1945) Ind Eng Chem 37:318; (b) Prater CO, Lago RM (1956) Adv Catal 8:293
33. (a) Stara I, Matolin V (1994) Surf Sci 131:99; (b) Matolin V, Gillet E (1990) Surf Sci 238:75; (c) El-Yakhloufi MH, Gillet E (1986) Catal Lett 17:11; (d) Gillet E, Chamnkhone S, Matolin V (1986) J Catal 97:437
34. Oh SH, Eickel CC (1991) J Catal 128:526